PROGRESS IN COLOR, COLORANTS AND COATINGS

available online @ www.pccc.icrc.ac.ir

Prog. Color Colorants Coat. 9 (2016), 173-181

Ministry of Science, Research and Technology
Institute for Color Science and Technology

Corrosion Behaviour of Nickel Coated AISI 316 Stainless Steel as a Function of Annealing Temperature

A. R. Grayeli Korpi *

Physics and Accelerators Research School, Nuclear Sciences and Technology Research Institute, P. O. Box: 11365-3486, Tehran, Iran.

ARTICLE INFO

Article history:
Received: 19 Apr 2016
Final Revised: 06 Jun 2016
Accepted: 11 Jun 2016
Available online: 11 Jun 2016

Keywords:
Ni thin films
Potentiodynamic
Stainless steel
Corrosion

ABSTRACT

AISI 316 stainless steels were coated with 250 nm Ni film by electron beam deposition and post-annealed at different temperatures with a nitrogen flow of 600 cm^3min^{-1} nitrogen. The prepared samples were corrosion tested in 1.0 M sulphuric acid solution using potentiodynamic technique. Crystallographic and morphological structure of the samples were analyzedanalysed by X-ray diffraction (XRD) and atomic force microscopy (AFM) respectively before corrosion test, and scanning electron microscope (SEM) after corrosion test. A clear correlation between the physical analyses (XRD, AFM and SEM) and the potentiodynamic results was is achieved. It is found that both surface roughness and the annealing temperature have important role on corrosion resistance performance of the samples produced in this work and the optimum results can be obtained at annealing temperature of 623 K for AISI 316 samples where both surface roughness and temperature (diffusion effect) have reached their critical values. Prog. Color Colorants Coat. 9 (2016), 173-181© Institute for Color Science and Technology.

1. Introduction

AISI 316 stainless steel is probably the most commonly used among all the stainless steels. It consists of an austenitic matrix and possesses good corrosion resistance in the most atmospheres and oxidizing acids. This alloy containsalloycontain iron, principally, and a minimum of 17% chromium. Chromium reacts with oxygen and moisture in the environment to form a protective, adherent and coherent oxide film that envelops the entire surface of the material [1, 2]. Exposing to a gaseous or aqueous environment, a thin and dense oxide layer may form to further restrain the penetration of corroding species into the surface of the material. Therefore, 316 stainless steel can achieve the characteristic of corrosion resistance inherently [3]. A variety of factors can influence the stability of this passive film, such as the film's chemical composition, temperature, exposure time in solution, film's structure and number of grain boundaries. It is also shown that the passive film formed on a stainless steel (SS) exposed to corrosive environment is Cr-enriched [3, 4].

Although chemical composition is a basic factor

*Corresponding author: grayli@ut.ac.ir

that affects the corrosion behaviour, a wide variety of surface modification methods of austenitic SSs such as gas nitriding, ion nitriding, physical vaporvapour deposition and ion implantation have been studied to improve corrosion properties [5-7]. Deposition processes under a controlled atmosphere, like physical vaporvapour deposition (PVD), have gained especial importance in new environmental protection awareness. Transition metal nitrides are the most common materials for PVD coating techniques. Owing to the important effects of microstructure and phase on corrosion properties, many researchers have focused their studies on the modification of microstructure and phases of stainless steels by adding some metals in their original compositions. Nickel and chromium are two metals which have received special attention. Another important method of improving surface hardness and corrosion resistance of stainless steels is nitrogen treatment which has attracted more attention in recent years, especially for austenitic stainless steels. It is observed that nitriding results in better corrosion resistance by forming multiple nitride phases [8, 9]. Due to their unique properties such as high hardness, high melting point, chemical stability, low electrical resistivity and high thermal conductivity, metal nitride coatings have gained considerable interest during the last decade. These coatings are used in a wide variety of applications.

In this work, nickel coating which was post-nitrided at different temperatures was used to improve the corrosion resistance of AISI 316 stainless steels that have many domestic and industrial applications in different atmospheres and media (e.g., acidic (HCl or H_2SO_4) [10-12] or chloride containing solutions [13-18] or combination of acidic and chloride containing solutions [19, 20]).

Hence, this study contains experiments which reveal the effect of annealing temperature on nano-structure (surface morphology) of each phase, and the associated corrosion behaviorbehaviour of the AISI 316 SSs, thus determining the optimal annealing temperature. One of the most important effects of heat treatment on the structure of the films is grooving effect. It is noticeable that when a metal is hot enough to permit appreciable atomic migration, a thermal groove will develop along the line where a grain boundary intersects the surface. The motivation for the formation of the groove is the tendency of the grain boundary to shrink in order to reduce its area and hence lowering its free energy [21]. The transport processes by which the groove may develop are evaporation, surface diffusion and volume diffusion that have been studied in UHV deposited Ni thin films [22], Cu films [23], Ti thin films [24] and Pt thin films [25].

2. Experimental

Commercial austenitic type 316 stainless steel sheets of 1 mm thickness were used in the form of square samples (18×18 mm^2). After thorough cleaning of the samples in ultrasonic bath with heated acetone and ethanol, respectively, they were held (mounted) on the substrate holder and positioned in the evaporation chamber.

Nickel (99.98% purity) films of 250 nm thickness were deposited on substrates, using electron beam evaporation (PVD-EB, E19A3 Edwards model, England) at room temperature with a base pressure of 2×10^{-7} mbar. at room temperature with a deposition rate of 0.1 Å/s. Film thickness was controlled by using a quartz crystal thickness monitor (Sigma Instruments, SQM-160, USA) positioned close to the substrate. Nominal composition of AISI 316 stainless steel used in this work and the abundance of each element is given in Table 1 [26].

Stainless steel substrates/plates were covered with a polyethylene sheet (as a protective medium against scratching and oxidation) by the producing factory. After cutting the substrates into desired size, the polyethylene sheets were removed by soaking the substrates in ethanol, and all the substrates were ultrasonically cleaned in heated acetone and ethanol, respectively. Post-annealing of the Ni films were performed at four different temperatures of 473, 623, 773, and 923 K in nitrogen environment with a flow rate of 600 cm^3min^{-1} (the atmosphere air of the annealing tube was flushed with argon gas several times before introducing nitrogen and heating the samples).

Table 1: Nominal composition and abundances (%) of different elements in AISI 316 stainless steels [25].

SS Type	Fe (%)	Cr (%)	Ni (%)	Mo (%)	Mn (%)	Si (%)	C (%)	P(%)	S (%)
SS(316)	62-71	16-18	10-14	2-3	2	1	0.08	0.045	0.03

Crystallographic structure of these films was obtained using a diffractometer (STOE STADI MP, Germany, CuKα radiation) with a step size of 0.01º and count time of 1.0 s per step, while the surface physical morphology, nanostructure and roughness were obtained by means of AFM analysis (Auto Probe Pc, Park Scientific Instrument, USA; in contact mode, with low stress silicon nitride tip of less than 200 Å radius and tip opening of 18°) and scanning electron microscope (LEO 440i, England).

Electrochemical behaviorbehaviour of the samples was evaluatedachieved using potentiodynamic method with a potentiostat coupled to PC (273A, EG & G, USA). In order to carry out the analysis, only an area of 1.0 ± 0.05 cm^2 was exposed to the acidic environment. The samples were polarized in 1 M H_2SO_4, a solution made of analytical grade reagent and double distilled water. A saturated calomel reference electrode (SCE) and a platinum counter electrode were used in three electrode setup. The samples were polarized from -400 mV vs to +400 mV vs. open circuit potential at a scan rate of 1 mV s^{-1}. The ends of the scans were selected after considering transpassive behaviorbehaviour in polarization curves. All the potentials presented in this work are as a function of SCE.

3. Results and discussions

3.1. Crystallographic and nanostructure nature of the films

Figure 1 shows, XRD patterns of the SS substrate, as deposited and post-annealed Ni/SS 316 films at four different temperatures in nitrogen atmosphere, respectively. In addition to four SS peaks, of course with lower intensity, the XRD pattern of the as deposited (i.e., Ni/SS) represented only the Ni(111) line of nickel (with reference to film ($2\theta = 44.521°$); JCPDS Card No.: 45-1027). At 473, 623 and 773 K annealing temperatures, with the flow of 473, 623 and 773 K, under nitrogen purging, ,films showed one peak which can be designated to Ni_3N(111), with reference to ($2\theta = 44.485°$); JCPDS Card No.: 10-0280. It can be observed that the intensity of this peak has its maximum at 623 K annealing temperature in Figure 1, which indicates that at this temperature highest amount of nickel nitride is formed compare to the rest of the samples. When the annealing temperature is increased to 923 K, two peaks of Ni_4N(222) and Ni_4N(320) are observed with reference to ($2\theta = 90.998°$ and $2\theta = 95.577°$); JCPDS Card No.: 36-1300, respectively. Moreover, the increase of intensity of SS peaks at this temperature relative to lower temperatures is in agreement with the grooving effect [27] which becomes activated due to the higher diffusion effects at higher temperatures, resulting in very thin layers in wide valleys between large grains. This is further discussed usingin the following paragraphs where the results of AFM analysis are presented.

3.2. AFM results

The AFM images of stainless steel, as deposited and annealed Ni/AISI316 samples are given in Figure 2, while surface roughness of the samples obtained from the AFM measurements are given in Table 2. Grain sizes are also obtained from the 2D images of the AFM results using the JMicroVision Code (Table 2). The results of AFM analysis of the samples produced in this work showed that by increasing the annealing temperature, due to the surface diffusion which is typically a thermally promoted phenomenon, larger grains are formed as a result of migration of smaller grains (with higher rate than larger grains) and their coalescence of these grains with each other and with larger grains. However, at very high temperatures where diffusion process is enhanced to a great deal, grooving effect usually takes place and very large grains are formed with deep and wide valleys between them which may extend to the substrate surface.

It can be observed that the deposited sample does not show any distinguished morphology when compared with the bare SS substrate (compare Figures 2(a) and 2(b)). The Ni/AISI316 sample annealed at 473

K (Figure 2(c)) shows needle like grains with slight increase in surface roughness relative to bare SS substrates and unheated samples (Table 2, columns 4 and 5). The distinguished difference between unheated and annealed sample at 473 K samples clearly shows the effect of annealing of the samples with flow of nitrogen (Figure 2(c)). Increasing the annealing temperature to 623 K produced a film with larger grains (Figure 2(d)) which is related to higher activation processes (diffusion effect). AFM image of the sample annealed at 773 K shows formation of even larger grains with some grooving effect enhanced diffusion effects (Figure 2(e)). Further increase of annealing temperature to 923 K produced somewhat larger grains with even deeper and wider grooves (Figure 2(f)).

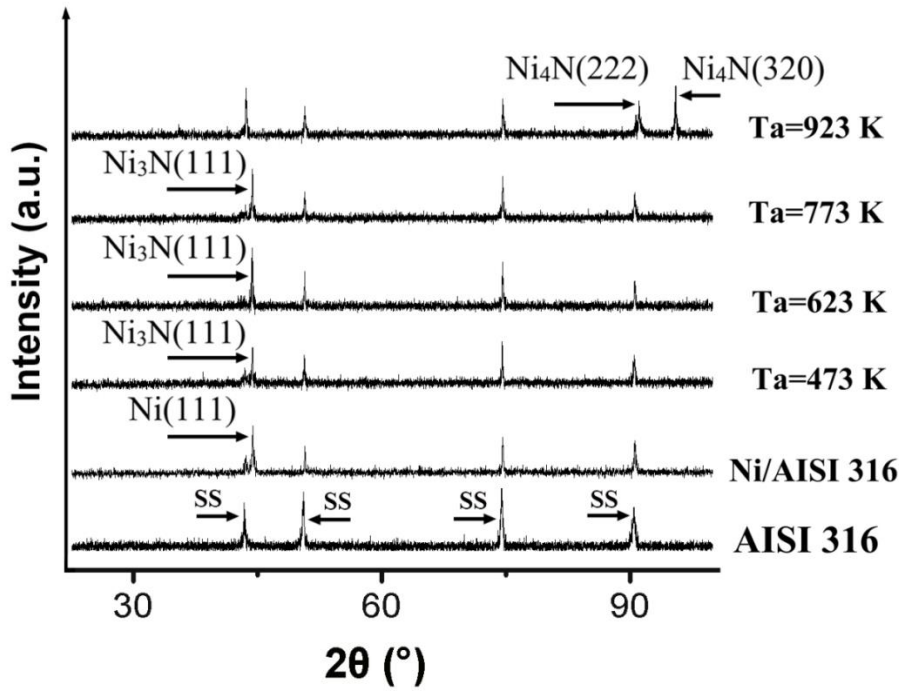

Figure 1: XRD Patterns of AISI 316 stainless steel and Ni/AISI 316 samples annealed at different temperatures with flow of nitrogen.

Table 2: The grain size, surface roughness and corrosion parameters of samples produced on AISI 316 substrates.

Sample		T_a (K)	AFM diameter (nm)	R_{ave} (Å)*	Rms (Å)*	Corrosion current density (μA cm^{-2})	Corrosion potential (V vs. SCE)	Passive current density (μA cm^{-2})
AISI 316	1	SS Untreated	---	35.77	37.85	91.3163	-0.4007	184.71
	2	Ni/SS Unheated	---	42.61	45.38	3.0953	-0.2613	9.97
	3	473	36.85	43.91	45.90	15.5991	-0.3057	32.35
	4	623	56.79	45.80	50.75	1.2735	-0.1102	8.09
	5	773	188.56	62.08	66.07	17.8238	-0.3459	205.47
	6	923	202.65	65.95	68.11	40.0867	-0.3327	80.17

R_{ave} instead of) average surface roughness ; Rms instead of) root mean square of surface roughness

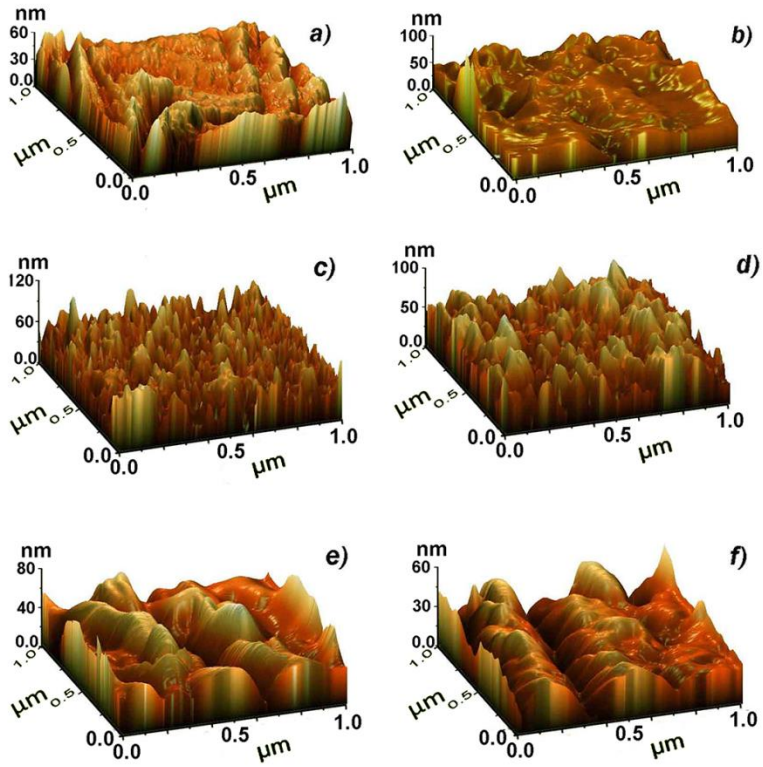

Figure 2: 3D AFM images of; a) AISI 316 stainless steel, b-e) Ni/AISI 316 samples annealed at different temperatures of 300, 473, 623, 773 and 923 K, respectively.

3.3. Polarization results

Potentiodynamic curves representing the bare stainless steel substrate, SS substrate coated with Ni thin film (unheated sample) and those annealed at different temperatures with flow of nitrogen are given in Figure 3. It can be observed that all these curves show active-passive behaviour. The electrochemical characteristics (i.e. corrosion current density, corrosion potential and passive current density) obtained from these curves are given in Table 2.

The polarization plot illustrates that the deposition of Ni on stainless steel substrate increases its resistance toagainst corrosion. A remarkable tendency to corrosion protection for the treated SS samples, with the polarization curves shifting towards lower corrosion current densities and higher corrosion potentials can be observed in Figure 4, such that for the sample annealed at 623 K, the optimum corrosion current density and corrosion potential are obtained as 1.2735 µA/cm^2 and -0.1102 V vs. SCE, respectively, while these quantities for bare AISI316 substrate are 91.3163 µA/cm^2 and -0.4007 Vvs. SCE. Furthermore, from the results in Figure 3 and Table 2 it can also concludedbe observed that the lowest value of the passive current density belongs to the sample annealed at 623 K.

3.4. SEM results

Surface morphology images of samples after corrosion test are presented in Figure 5. Comparison of Figure 5(a) obtained from uncoated stainless steel with those of samples coated with Ni film and annealed with flow of nitrogen at different temperatures (Figures 5(b-f) clearly show that the latter samples have remained more intact than the bare stainless steel. This may be qualitatively achieved by the extent of damage occurred on these samples after corrosion test. In addition, it can also be observed that the SEM image of the sample annealed at 623 K (Figure 5(c)) shows the least amount of corrosion effects on its surface consistent with polarization and AFM results which areis carefully investigated in detail in section 4. bellow. However, other samples produced at higher and lower annealing temperatures show signs of cracks or pitted areas which are formed as a result of corroding test. Images with of 1 micron scale in Figure 5 show the details of surface defects in of various samples.

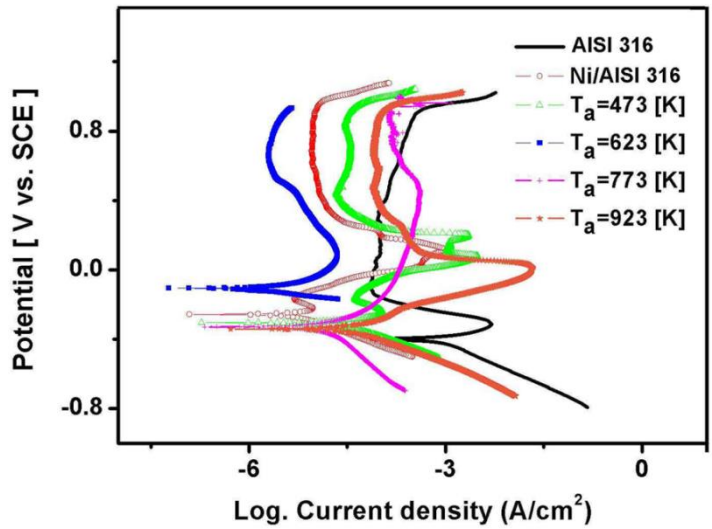

Figure 3: Potentiodynamic polarization curves for stainless steel and deposited sample with nickel thin film annealed at different temperatures.

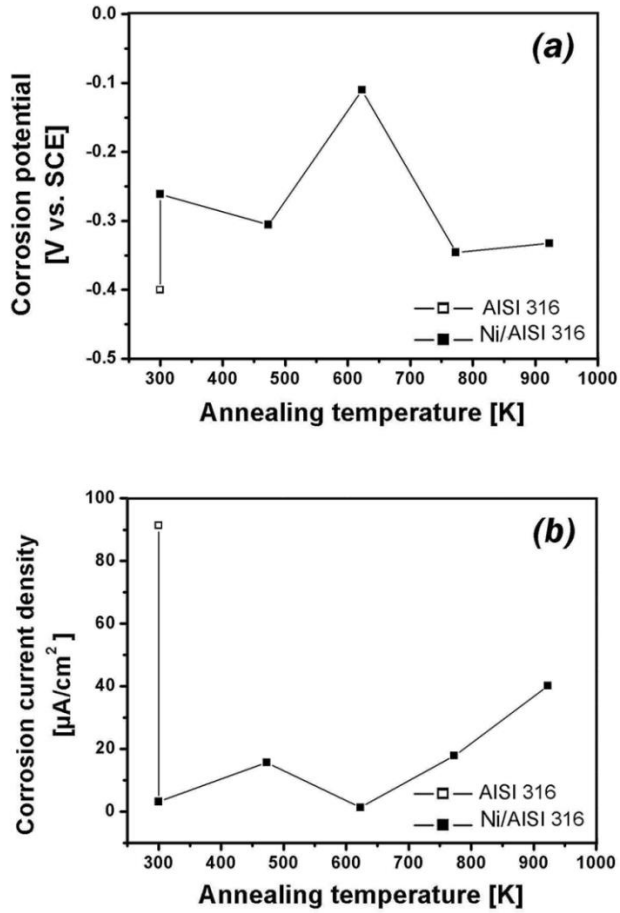

Figure 4: Variations of; a) corrosion potential, b) corrosion density as a function of annealing temperature for AISI 316 and Ni/SS 316 samples annealed at different temperatures with flow of nitrogen.

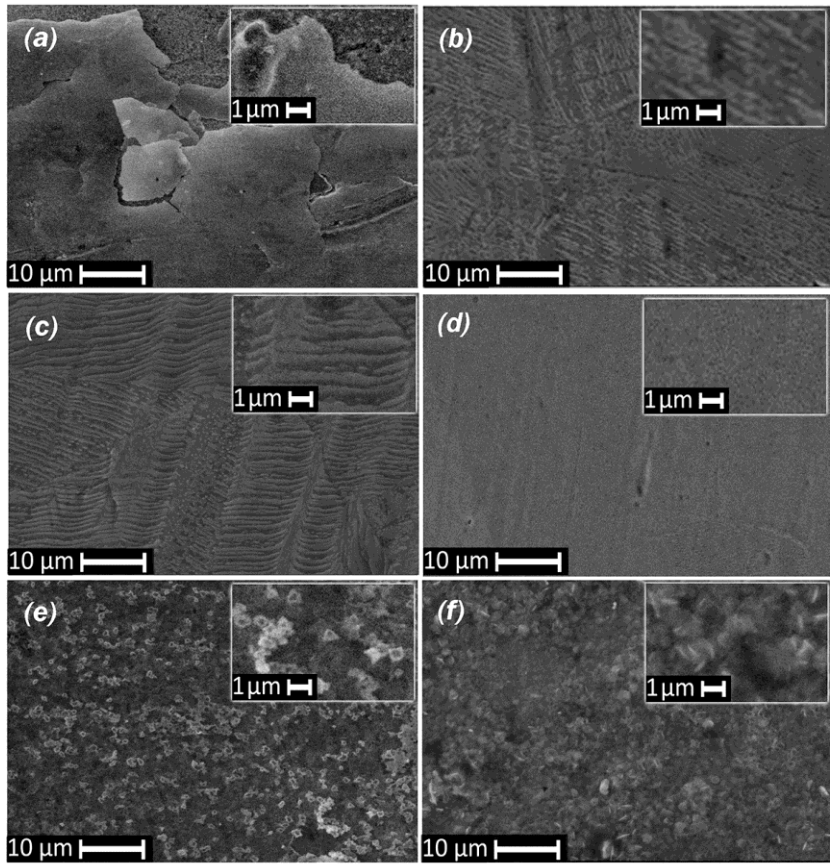

Figure 5: SEM images of; a) AISI 316, b-f) Ni/AISI 316 annealed at different temperatures of 300, 473, 623, 773 and 923 K, respectively, with flow of nitrogen after the corrosion test

3.5. Discussion

The AFM images and surface roughness results as well as the changes observed in the intensity of the XRD peaks and also phase transformation at highest temperature of 923 K may be used to obtain a useful correlation with the results obtained from the potentiodynamic tests.

According to the explanation of the grooving effect [27], the diffusion processes are enhanced by increasing the temperature, and crystallites with relatively lower surface energies in different areas of the substrate diffuse into each other to produce larger grains withof different phases of nickel nitride, which are separated from each other by grooves between them. The XRD results in Figure 1 confirm the latter statement as the nickel nitride phase changes from Ni_3N(111), obtained at lower temperatures, to Ni_4N(320) and Ni_4N(222) at 923 K annealing temperature and as previously mentioned, due to formation of deep (thinner film coating on the SS substrate) and wide grooves, the diffraction lines of stainless steel substrate appear again with higher intensity in comparison to the lower temperature samples.

It has observed by many researchers [28, 29] that larger grains/columns grow on rough surfaces while non-columnar/needle like grains grow on smooth surfaces, and the similarity results inis resulted to the enhanced diffusion effect at higher temperatures.

It was observed that the surface roughness increased with annealing temperature, since by increasing the temperature, larger grains are formed with wider and deeper valleys between them. Hence, the film thickness at valleys becomes thinner (in extreme case these valleys form grooves and the valleys/grooves themselves may extend to the surface of the substrate), which results in exposure of larger surface area (effective surface) to the corroding media. This, in turn, causes an increase in the corrosion reaction rate. During the process of these chemical reactions, electrons are released and an electric current formed. Although surface roughness increases with temperature, but at the same time the diffusion process

also activates at the same time and the small grains coalesce. All the results (e.g., corrosion current density and corrosion potential) show the existence of critical values for both surface roughness and the annealing temperature which produced the optimum results (i.e., at 623 K annealing temperature). At this temperature, although larger grains are formed due to diffusion effect, the valleys/boundaries between them still form a thick film layer which protects the sample against corrosion. While these areas become thinner at higher temperatures, these areas become thinner and the sample becomes more susceptible to the corroding media. The better behaviorbehaviour of AISI 316 at higher temperatures of 773 K and 923 K (i.e., lower corrosion currents) may be related to the 2-3% higher Mo content in the composition of AISI 316 as at these temperatures due to high diffusion rate, some grooves with deep and wide structure are formed between large grains which may extend to the substrate surface. Hence at these areas, the extra Mo acts as a protecting agent. The XRD results also show that the intensity of $Ni_3N(111)$ is highest at this temperature, sohence it can also be concluded that the volume of nickel nitride formed on this sample is more than those produced at lower and higher temperatures. Therefore, all the above discussions confirm showthe existence of a correlation between the reported results in this work.

4. Conclusion

The corrosion behaviorbehaviour of AISI316 type stainless steel was studied by deposition of 250 nm Ni coatings and further annealing the coated samples at different temperatures with flow of nitrogen, hence producing nickel nitride coatings on stainless steel. Potentiodynamic polarization tests were implemented to measure the corrosion resistance of the films which were carried out in 1.0 M sulphuric acid solution. The highest corrosion resistance was achieved at 623 K annealing temperature with corrosion current densities of 1.2735 $\mu A/cm^2$.

XRD and AFM analyses were used for determination of crystallographic and morphological structure of the samples before corrosion test while SEM was implemented after the corrosion test. All investigations showed a clear correlation between the physical analyses and the potentiodynamic results. It is shown that two factors have the prominent role in the corrosion resistance of the samples produced in this work, namely, surface roughness and the annealing temperature (diffusion effect). and it was also found that there exist a combination of critical surface roughness and a critical temperature that produce the optimum result (i.e., 623 K annealing temperature with associated surface roughness in this work; given in Table 2).

5. References

1. J. G. Parr, A. Hanson, Stainless Steel, ASM International, Metals Park, OH, USA, 1986, 63-88.
2. A. I. M. Bernstin, Handbook of Stainless Steels, McGraw-Hill, New York, USA, 1977, 15.1-15.6.
3. R. M. Davison, T. DeBold, M. J. Johnson, Metals Handbook, ASM International, Metals Park, OH, USA, 1980, 550-565.
4. D. Stoychev , P. Stefanov , D. Nicolova , I. Valov, Ts. Marinova, Chemical composition and corrosion resistance of passive chromate films formed on stainless steels 316 L and 1.4801, *Mater. Chem. Phys.*, 73(2002), 252-258.
5. A. Neville , F. Reza , S. Chiovelli , T. Revega, Corrosion and synergy in a WC Co CrWC Co Cr HVOF thermal spray coating-understanding their role in erosion–corrosion degradation, *Wear*, 259(2005), 181-195.
6. P. Saravanan, V. S. Raja , S. Mukherjee, Effect of plasma immersion ion implantation of nitrogen on the wear and corrosion behavior of 316LVM stainless steel, *Surf. Coat. Technol*,. 201(2007), 8131-8135.
7. A. R. Grayeli Korpi, Kh. M. Bahmanpour, Influence of nitrogen ion implantation on the structure and corrosion resistance of stainless steel substrates coated with Ni nanolayer, *Prog. Color Colorants Coat.*, 9(2016), 77-83.
8. V. Vignal , N. Marya, P. Ponthiaux , F. Wenger, Influence of friction on the local mechanical and electrochemical behaviour of duplex stainless steels, *Wear*, 261(2006), 947-953.
9. C. Garcia, F. Martin , Y. Blanco, M. P. de Tiedra, M. L. Aparicio, Corrosion behaviour of duplex stainless steels sintered in nitrogen, *Corros. Sci.*, 51(2009), 76-86.

10. J. H. Potgieter, P. A. Olubambi, L. Cornish, C. N. Machio, M. Sherif El-Sayed, Influence of nickel additions on the corrosion behaviour of low nitrogen 22% Cr series duplex stainless steels, *Corros. Sci.*,50(2008), 2572-2579.
11. H. Baba , T. Kodama, Y. Katada, Role of nitrogen on the corrosion behavior of austenitic stainless steels, *Corros. Sci.*, 44(2002), 2393-2407.
12. B. R.Tzaneva, L. B. Fachikov and R. G. Raicheff, Pitting corrosion of Cr–Mn–N steel in sulfuricsulphuric acid media, *J. Appl. Electrochem.*, 36(2006), 347-353.
13. Y. Fu, X. Wu, H. En-Hou, W. Ke, K.Yang,Z. Jiang, Effects of nitrogen on the passivation of nickel-free high nitrogen and manganese stainless steels in acidic chloride solutions *Electrochim. Acta.*, *54*(2009), 4005-4014.
14. R. Merello, F. J. Botana, J. Botella, M. V. Matres,M. Marcos, Influence of chemical composition on the pitting corrosion resistance of non-standard low-Ni high-Mn–N duplex stainless steels, *Corros. Sci.*, 45(2003), 909-921.
15. C. M Tseng, H. Y Liou, W. T Tsai, The influence of nitrogen content on corrosion fatigue crack growth behavior of duplex stainless steel, *J. Mater. Sci. Eng. A*, 344(2003), 190-200.
16. J. W. Park, V. Shankar Rao, H. S. Kwon, Effects of Nitrogen on the RepassivationBehavior of Type 304L Stainless Steel in Chloride Solution, *Corrosion.*, 60(2004), 1099-1103.
17. H. Y. Ha, H. S. Kwon, Effects of Cr2N on the pitting corrosion of high nitrogen stainless steels, *Electrochim. Acta*,. 52(2007) 2175-2180.
18. U. KamachiMudali, P. Shankar, S. Ningshen, R. K. Dayal,H. S. Khatak, B. Raj, On the pitting corrosion resistance of nitrogen alloyed cold worked austenitic stainless steels, *Corros. Sci.*, 44(2002), 2183-2198.
19. H. Baba,Y. Katada, Effect of nitrogen on crevice corrosion in austenitic stainless steel, *Corros. Sci.*, 48(2006), 2510-2524.
20. Y. X. Qiao, Y. G. Zheng, W. Ke, P. C. Okafor, Electrochemical behaviour of high nitrogen stainless steel in acidic solutions, *Corros. Sci*,. 51(2009), 979-986.
21. W. W. Mullins, The effect of thermal grooving on grain boundary motion, *Acta metal.*, 6(1958), 414-427.
22. F. Maghazeii, H. Savaloni, M. Gholipour-Shahraki, The influence of growth parameters on the optical properties and morphology of UHV deposited Ni thin films, *Optic Commun*, 281(2008, 4687-4695
23. S. H. Kang, Y. S. Obeng, M. A. Decker, M. Oh, S. M. Merchant, S. K. Karthike, C. S. Seet, A. S. Oates, Effect of Annealing on the Surface Microstructural Evolution and the Electromigration Reliability of Electroplated Cu Films, *J. Elect. Mater.*, 30(2001), 1506-1511.
24. M. Firouzi-Arani, H. Savaloni, M. Ghoranneviss, Dependence of surface nano-structural modifications of Ti implanted by N^+ ions on temperature, *Appl. Surf. Sci*, 256(2010), 4502-4511
25. U. Schmid, The impact of thermal annealing and adhesion film thickness on the resistivity and the agglomeration behavior of titanium/platinum thin films, *J. Appl. Phys.*, 103 (2008), 054902- 054902.
26. J. R. Davis, Stainless Steels ASM Specialty Handbook, ASM International, OH, USA, 1996, pp. 22-24.
27. D.E. Aspnes, E. Kinsbron, D. D. Bacon, Optical properties of Au: Sample effects, *Phys. Rev. B: Condens. Matter Mater. Phys.*, 21(1980), 3290-3299.
28. H. Savaloni, M. Gholipour-Shahraki, Structural characteristics in UHV deposited Ti thin film, *Nanotechnology*, 15(2004), 311-319.
29. C.–O. A. Olsson, D. Landolt, Passive films on stainless steels-chemistry, structure and growth, *Electrochim. Acta.*, 48(2003), 1093-1104.

How to cite this article:
A. R. Grayeli Korpi, Corrosion Behaviour of Nickel Coated AISI 316 Stainless Steel as a Function of Annealing Temperature, Prog. Color Colorants Coat., 9 (2016) 173-181.